평면 뼈대구조물의 큰 변형에 대한 비선형 유한요소의 정식화

A Finite Element Nonlinear Formulation for Large Deformations of Plane Frames

윤 영 묵*
Yun, Young-Mook
박 문 호**
Park, Moon-Ho

요 약

평면 뼈대구조물의 매우 큰 변형에 대하여 정확한 비선형 유한요소의 정식화 과정을 나타내었다. 유한요소의 구성은 변화되는 재료의 기준 물성치에 근거를 두고 형성하였으며 매우 큰 변형을 받는 재료의 성질을 명확하게 특성지어 진응력-변형율 관계식을 직접 적용할 수 있도록 하였다. 큰회전과 작은 변형율을 받는 문제들을 형성하기 위하여 Co-rotation 접근 방법을 사용하였다. 큰 변형을 일으키는 요소의 문제를 해결하기 위하여 직선보 형태의 유한요소를 사용하였으며 개개의 유한요소의 정식화는 축방향력의 영향을 고려하여 미소처짐보이론을 바탕으로 형성하였다. 본 연구에서 형성된 큰 변형에 대한 비선형 유한요소의 타당성을 확인하기 위해 몇몇 수치해들을 해석하고 검토하였다.

Abstract

An explicit finite element nonlinear formulation for very large deformations of plane frame structures is developed. The formulation is based on an updated material reference frame and hence a true stress-strain relationship can be directly applied to characterize the properties of material which is subjected to very large deformations. In the formulation, a co-rotational approach is applied to deal with the large rotations but small strain problems. Straight beam element is considered when the strain of an element is large. The element formulation is based on the small deflection beam theory but with the inclusion of the effect of axial force. The element equations are constructed in an element local coordinate system which rotates and translates with the element, and then transformed to the global coordinate system. Several numerical examples are analyzed to validate the presented formulation.

* Post-Doctoral Researcher, School of Civil Engineering, Purdue University
** Professor, Dept. of Civil Engineering, Kyungpook National University

이 논문에 대한 토론을 1995년 6월 30일까지 본 학회에 보내주시면 1995년 12월호에 그 결과를 게재하겠습니다.

1. INTRODUCTION

The possibility of practical analysis of structures subjected to large deformation has progressed substantially during recent years. To enable general large deformation analysis the development of versatile geometric and material nonlinear finite element is in much need.

General theoretical formulations and computational techniques for the geometrical nonlinear analysis of frame structures have been extensively studied. One of the most popular formulations is Lagrangian approach within a finite elelement framework. Other formulations of the Lagrangian type approaches are possible, depending on the way in which the deformations are specified. There are, in general, two main types of Lagrangian approaches which are commonly used in geometrically nonlinear analysis.

The first type is the Total Lagrangian Formulation[1-7], where the deformation of the element is measured from its own original reference frame. Any subsequent deformation of the element will also refer to the same reference frame. This formulation procedure is easy to implement as calculations are straightforward. However, a major disadvantage of using this procedure is that it is not possible to distinguish the rigid body motion of the element explicitly from its local deformation. This leads to an erroneous description of the equilibrium path except for problems with small or moderate rotations and deflections.

The second type is the Updated Lagrangian Formulation,[2,4,8-10] where the current configuration of the element at any time is taken as the reference frame. In this way, the rigid body motion of the element can be separated from its local deformation. Although this method gives a more accurate description of the displacement field of both elements and structures, the effort involved in calculating the local element deformations at any stage of loading is enormous. Moreover, in developing a consistent set of equilibrium equations for the incremental analysis, a large number of matrix operations is necessary when the tangent stiffness matrix is transformed from its local to global axes. For this reason, the modified updated Lagrangian formulation known as Partially Updated Lagrangian Formulation has been developed. This modified formulation makes use of the concept of the rigid-convected coordinates approach, as used in the updated Lagrangian formulation. A major difference of the modified formulation, as compared with the updated Lagrangian formulation, is that the coordinates of each element are updated once only at the beginning of every load step. The numerical manipulations within each load step are then performed in a total Lagrangian formulation manner. This type of formulation takes advantage of the simplicity of the total Lagrangian formulation as well as the accuracy inherent in updated Lagrangian formulation.

In addition to the Lagrangian formulations, co-ratational formulations have been developed for the analysis of the structures which experience large displacements and large rotations.[11-21] In the derivation of the equations of the co-rotational formulation, unlike Lagrangian Formulations in which the finite element equations are obtained by discretization of equalibrium equations established for the whole continuum, attention is focused on a single finite element of the body. In the formulation, each element is associated with a local cartesian element coordinate system that rotates and translates with the element but does not deform with the element.

Most of the current large deformation algor-

ithms based on the Lagrangian formulations, however, show serious numerical limitations. Typically, the solutions become unstable either at a certain point when the iterations fail to converge or the algorithms fail to handle the negative deformation gradient when the deformation becomes very large. A more serious problem common to all formulations is that the definitions of stress and strain, their increments and the constitutive equations include geometrical couplings, and hence correlating them to the material testing data becomes difficult.

In this paper, an finite element nonlinear formulation for very large deformations of plane frame structures, which has the capability of handling large geometrical changes whithout the need for lengthy iterations and handling the material data more accurately, is developed. The formulation is based on an updated material reference frame and hence true stress-strain relationship can be directly applied to correctly characterize properties of materials which undergo nonlinear deformations. In the formulation, a co-rotational approach is applied to deal with the large rotations but small strain problems. Straight beam element is considered when the strain of an element is large. The element formulation is based on the small deflection beam theory but with the inclusion of the effect of axial force. The element equations are constructed in an element local coordinate system which rotates and translates with the element, and then transformed to the global coordinate system. The element external nodal forces are evaluated using the total deformational nodal rotations in the body attached coordinate. For the numerical solution, an explicit incremental numerical procedure is adopted. Gaussian numerical integration is used to evaluate element integral for stiffness

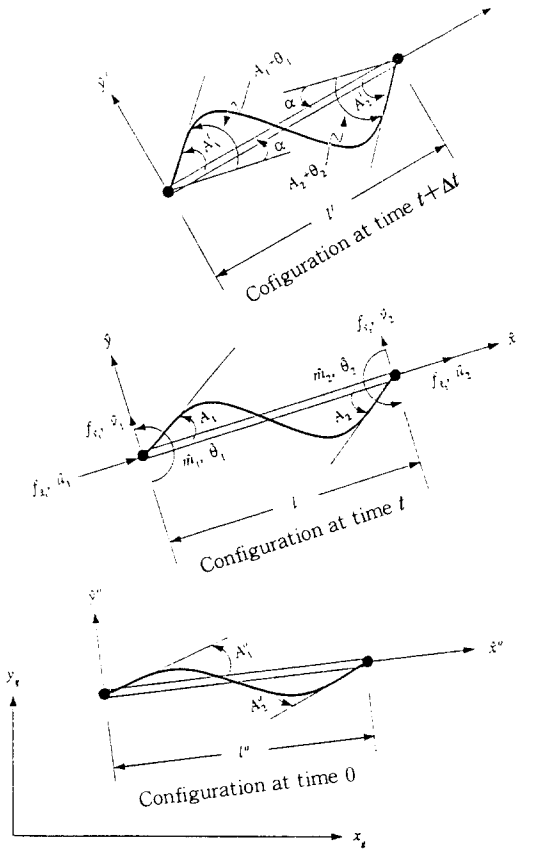

Figure 1 The Body Attached Coordinate and Deformed Frame Member

matrices and element external nodal forces. Several numerical examples of beams and frames with large deformations are presented.

2. FINITE ELEMENT FORMULATION

In this analysis, the element equations are formulated in the body attached coordinate as shown in Figure 1. The system equations are obtained from the assemblage of individual element equations. The normal strain of an element is sum of axial and bending strains. The bending strain is evaluated using the Euler-Bernoulli hypothesis. The element internal and external nodal forces are obtained from the vir-

tual work principle. The element stiffness matrix is established from the derivative of the element internal nodal force vector with respect to the nodal displacement vector.

2.1 Kinematics of Individual Member

If the undeformed and deformed axes of the beam member are assumed to be the linear interpolation for the axial and cubic interpolation for bending displacement in the body attached coordinates, the axial and bending displacements of the beam axis in the configuration at time t may be given by

$$\hat{u} = \underline{N}_r^T \underline{\hat{u}}_r \tag{1}$$

$$\hat{v} = \underline{N}_b^T \underline{\hat{u}}_b \tag{2}$$

where $\underline{N}_r^T$ and $\underline{N}_b^T$ are respectively the transposes of displacement shape functions for a rod and a beam element :

$$\underline{N}_r^T = [\, N_{r1} \quad N_{r2} \,] \tag{3}$$

$$\underline{N}_b^T = [\, N_{b1} \quad N_{b2} \quad N_{b3} \quad N_{b4} \,] \tag{4}$$

where,

$$N_{r1} = 1 - \frac{\hat{x}}{l}, \quad N_{r2} = \frac{\hat{x}}{l}$$

$$N_{b1} = \frac{1}{l^3}(2\hat{x}^3 - 3\hat{x}^2 l - l^3), \quad N_{b2} = \frac{1}{l^3}(\hat{x}^3 l - 2\hat{x}^2 l^2 - \hat{x} l^3)$$

$$N_{b3} = \frac{1}{l^3}(-2\hat{x}^3 + 3\hat{x}^2 l), \quad N_{b4} = \frac{1}{l^3}(\hat{x}^3 l - \hat{x}^2 l^2)$$

In eqns (1) and (2), $\underline{\hat{u}}_r$ and $\underline{\hat{u}}_b$ are respectively the axial and bending displacement vectors :

$$\underline{\hat{u}}_r^T = [\, \hat{u}_1 \quad \hat{u}_2 \,] \tag{5}$$

$$\underline{\hat{u}}_b^T = [\, \hat{v}_1 \quad \hat{\theta}_1 \quad \hat{v}_2 \quad \hat{\theta}_2 \,] \tag{6}$$

where, $\hat{u}_r$, $\hat{v}_i$ and $\hat{\theta}_i (i=1,2)$ are respectively the axial nodal displacement, bending nodal displacement and nodal rotations at nodes i.

The normal strain for any point of the cross section of the member may be written as

$$\varepsilon = \varepsilon_r + \varepsilon_b \tag{7}$$

where ε_r is the axial strain and ε_b is the bending strain. Since the axial strain from the configuration at time t to the configuration at time $t+\Delta t$ is generally small, the linear term only may be taken :

$$\varepsilon_r = \frac{d\hat{u}}{d\hat{x}} \tag{8}$$

From the deformed configuration of the beam shown in Figure 2, the axial displacement may be related to the transverse displacement by

$$\hat{u} = -t\frac{d\hat{v}}{d\hat{x}} \tag{9}$$

where t is the distance from the axis of centroid to the measured point on the cross section. Substituting eqn (9) into eqn (8) and using the Euler-Bernoulli hypothesis, i.e, cross-

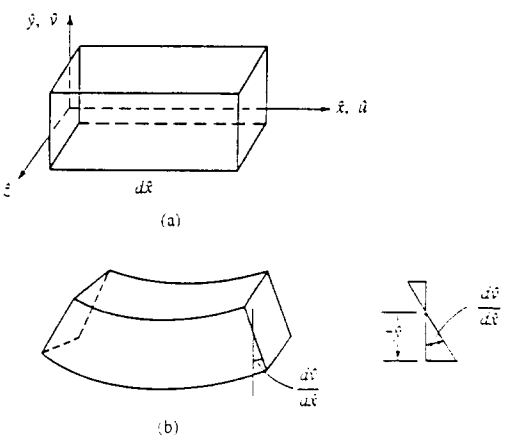

Figure 2 Beam Element a) before Deformation and (b) after Deformation

sections of the beam that are planar before bending deformation remain planar after deformation, the bending strain with linear term only is expressed as

$$\varepsilon_b = -t\frac{d^2\hat{v}}{d\hat{x}^2} \tag{10}$$

2.2 Deformational Rotations and Geometry Shape Function

Let A_i, x_{gi} and $y_{gi}(i=1,2)$ be respectively the total deformed nodal angles including the initial nodal angles and global nodal coordinates for a single element in the configuration at time t, and $\underline{d}_e$ be the nodal displacement vector of a single element extracted from the incremental displacement vector of the system of the equations, and given by

$$\underline{d}_e^T = [\,u_1 \;\; v_1 \;\; \theta_1 \;\; u_2 \;\; v_2 \;\; \theta_2\,] \tag{11}$$

where $\hat{u}_i$, $\hat{v}_i$ and $\hat{\theta}_i(i=1,2)$ are the nodal displacements and rotations in the global coordinate. Then the nodal coordinates x_{gi}' and y_{gi}' of the element and the total deformed nodal angles A_i' in the configuration at time $t+\Delta t$ are, respectively, obtained by

$$x_{gi}' = x_{gi} + u_i \tag{12}$$

$$y_{gi}' = y_{gi} + v_i \tag{13}$$

$$A_i' = A_i + \theta_i - \alpha \tag{14}$$

where α is the angle of rigid body rotation measured from the configuration at time t to the configuration at time $t+\Delta t$:

$$\alpha = \sin^{-1}\left[\frac{(x_{c2}-x_{c1})(v_2-v_1)-(y_{c2}-y_{c1})(u_2-u_1)}{l\,l'}\right] \tag{15}$$

In a similar manner, the nodal coordinates x_{gi} and y_{gi} may be evaluated using the same process of obtaining x_{gi}' and y_{gi}'.

The geometry shape of beam element in the configuration at time $t+\Delta t$ can be approximated using eqn(2), in which nodal angles A_i are used instead of $\hat{\theta}_i(i=1,2)$:

$$\hat{y}(\hat{x}') = N_{b1}\hat{v}_1 + N_{b2}A_1 + N_{b3}\hat{v}_2 + N_{b4}A_2 \tag{16}$$

where $N_{bi}(i=1,2,3,4)$ and $\hat{v}_i(i=1,2)$ are respectively the displacement shape functions and the transverse nodal displacements of a beam element in local coordinates at time t.

2.3 Element Internal Nodal Forces

The element internal nodal forces are obtained from the virtual work principle. The element nodal force vector is divided into axial and bending nodal force vectors as

$$\underline{\hat{F}}_r^T = [\,F_{x1} \;\; F_{x2}\,] \tag{17}$$

$$\underline{\hat{F}}_b^T = [\,F_{y1} \;\; \hat{M}_1 \;\; F_{y2} \;\; \hat{M}_2\,] \tag{18}$$

where F_{xi} F_{yi} and $\hat{M}_i(i=1,2)$ are respectively the axial nodal forces, the lateral nodal forces and moments at nodes i. The nodal force vectors $\underline{\hat{F}}_r$ and $\underline{\hat{F}}_b$ can be evaluated by introducing nodal virtual displacements $\delta\,\underline{\hat{u}}_r$ and $\delta\,\underline{\hat{u}}_b$ and equating the work done by the axial nodal force $\underline{\hat{F}}_r$ and bending nodal force $\underline{\hat{F}}_b$ going through the virtual displacements $\delta\,\underline{\hat{u}}_r$ and $\delta\,\underline{\hat{u}}_b$ to the work done by the internal stress σ going through the virtual strain $\delta\varepsilon=\delta\varepsilon_r+\delta\varepsilon_b$ along the deformed beam axis :

$$\int_V \sigma\,\delta\varepsilon\,dV = \delta\underline{\hat{u}}_r^T\underline{\hat{F}}_r + \delta\underline{\hat{u}}_b^T\underline{\hat{F}}_b \tag{19}$$

where V is the volume of the beam element.

If an initial axial force S acts in the local $\hat{x}$ direction, another internal virtual work caused by initial axial force S must be included in the

left side of eqn (19). Then eqn (19) becomes

$$\int_V \sigma\,\delta\varepsilon\,dV = \int_0^S \left(\frac{d\hat{v}}{d\hat{x}}\right)\delta\left(\frac{d\hat{v}}{d\hat{x}}\right)d\hat{x} = \delta\underline{\hat{u}}_r^T\,\underline{\hat{F}}_r + \delta\underline{\hat{u}}_b^T\,\underline{\hat{F}}_b \qquad (20)$$

From eqns (1), (2), (8) and (10), the variation $\delta\varepsilon_r$, $\delta\varepsilon_r$ and $\delta\left(\frac{dv}{dx}\right)$ are given by

$$\delta\varepsilon_r = \delta\left(\frac{d(\underline{N}_r^T\,\underline{\hat{u}}_r)}{d\hat{x}}\right) = \underline{N}_{r,x}^T\,\delta\underline{\hat{u}}_r \qquad (21)$$

$$\delta\varepsilon_b = \delta\left(-t\,\frac{d^2(\underline{N}_b^T\,\underline{\hat{u}}_b)}{d\hat{x}^2}\right) = -t\,\underline{N}_{b,xx}^T\,\delta\underline{\hat{u}}_b \qquad (22)$$

$$\delta\left(\frac{d\hat{v}}{d\hat{x}}\right) = \delta\left(\frac{d(\underline{N}_b^T\,\underline{\hat{u}}_b)}{d\hat{x}}\right) = \underline{N}_{b,x}^T\,\delta\underline{\hat{u}}_b \qquad (23)$$

where $\underline{N}_{r,x}^T$, $\underline{N}_{b,x}^T$ and $\underline{N}_{b,xx}^T$ are respectively the transposes of the single and double derivatives of axial and bending displacement shape functions for a rod and a beam element with respect to $\hat{x}$:

$$\underline{N}_{r,x}^T = [\,N_{r1,x}\;\;N_{r2,x}\,] \qquad (24)$$

$$\underline{N}_{b,x}^T = [\,N_{b1,x}\;\;N_{b2,x}\;\;N_{b3,x}\;\;N_{b4,x}\,] \qquad (25)$$

$$\underline{N}_{b,xx}^T = [\,N_{b1,xx}\;\;N_{b2,xx}\;\;N_{b3,xx}\;\;N_{b4,xx}\,] \qquad (26)$$

By substituting eqns (21), (22) and (23) into eqn (20), the left side of the eqn (20) becomes

$$l.s. = \delta\underline{\hat{u}}_r^T\int_V \sigma\,\underline{N}_{r,x}\,dV + \delta\underline{\hat{u}}_b^T\left[-\int_V \sigma\,t\,\underline{N}_{b,xx}\,dV + \int_0^t S\,\underline{N}_{b,x}\,\underline{N}_{b,x}^T\,\underline{\hat{u}}_b\,d\hat{x}\right] \qquad (27)$$

Equating eqn (27) to the right side of eqn (20) yields the internal nodal force vectors as

$$\underline{\hat{F}}_r = \int_V \sigma\,\underline{N}_{r,x}\,dV \qquad (28)$$

$$\underline{\hat{F}}_b = -\int_V \sigma\,t\,\underline{N}_{b,xx}\,dV + \int_0^t S\,\underline{N}_{b,x}\,\underline{N}_{b,x}^T\,\underline{u}_b\,d\hat{x} \qquad (29)$$

2.4 Element Stiffness Matrix

The element stiffness matrix in the configuration at time t can be obtained by differentiating the element nodal force vectors $\underline{\hat{F}}_r$ and $\underline{\hat{F}}_b$ with respect to element nodal displacement vectors $\underline{\hat{u}}_r$ and $\underline{\hat{u}}_b$, and expressed as

$$\underline{\hat{K}} = \begin{bmatrix} \frac{\partial\underline{\hat{F}}_r}{\partial\underline{\hat{u}}_r} & \frac{\partial\underline{\hat{F}}_r}{\partial\underline{\hat{u}}_b} \\ \frac{\partial\underline{\hat{F}}_b}{\partial\underline{\hat{u}}_r} & \frac{\partial\underline{\hat{F}}_b}{\partial\underline{\hat{u}}_b} \end{bmatrix} = \begin{bmatrix} \underline{\hat{K}}_{rr} & \underline{\hat{K}}_{rb} \\ \underline{\hat{K}}_{br} & \underline{\hat{K}}_{bb} \end{bmatrix} \qquad (30)$$

The derivatives of the stress σ with respect to $\underline{\hat{u}}_r$ and $\underline{\hat{u}}_b$ are obtained by using the chain rule of differentiation as

$$\frac{\partial\sigma}{\partial\underline{\hat{u}}_r} = \frac{\partial\sigma}{\partial\varepsilon}\,\frac{\partial\varepsilon}{\partial\underline{\hat{u}}_r} = {}^tE\,\underline{N}_{r,x}^T \qquad (31)$$

$$\frac{\partial\sigma}{\partial\underline{\hat{u}}_b} = \frac{\partial\sigma}{\partial\varepsilon}\,\frac{\partial\varepsilon}{\partial\underline{\hat{u}}_b} = {}^tE\,t\,\underline{N}_{b,xx}^T \qquad (32)$$

where ${}^tE\left(=\frac{\partial\sigma}{\partial\varepsilon}\right)$ is the updated Young's modulus of elasticity[22].

Using eqns through (28) to (32), the submatrices of $\underline{\hat{K}}$ in eqn (30) are expressed as

$$\underline{\hat{K}}_{rr} = \int_A\int_C {}^tE\,\underline{N}_{r,x}\,\underline{N}_{r,x}^T\,dA\,dC \qquad (33)$$

$$\underline{\hat{K}}_{rb} = \underline{\hat{K}}_{br}^T = -\int_A\int_C {}^tE\,\underline{N}_{r,x}\,\underline{N}_{b,xx}^T\,t\,dA\,dC \qquad (34)$$

$$\underline{\hat{K}}_{bb} = \int_A\int_C {}^tE\,\underline{N}_{b,xx}\,\underline{N}_{b,xx}^T\,t^2\,dA\,dC - \int_0^t S\,\underline{N}_{b,x}\,\underline{N}_{b,x}^T\,d\hat{x} \qquad (35)$$

where A and C are respectively the cross section area and the arc length of the beam element in the configuration at time t. Since the derivatives of displacement shape functions used in equations for submatrices of $\underline{\hat{K}}$ are all functions of $\hat{x}$, the are length of beam segment, dC, need to be changed by a function of $\hat{x}$ for the evaluation of element integral :

$$dC = J\,d\hat{x} = [\,1 + (\frac{d\hat{y}}{d\hat{x}})^2\,]^{\frac{1}{2}}\,d\hat{x} \tag{36}$$

where J is Jacobian and $(\frac{dy}{dx})$ is the derivative of the geometry shape function $\hat{y}(\hat{x})$ in the configuration at time t.

By substituting the derivatives of displacement shape functions and eqn (36) into eqns (33), (34) and (35) and by considering an element with rectangular cross section of width b and height h, the submatrices of $\hat{\underline{K}}$ are written explicitly by

$$\hat{\underline{K}}_{rr\ [2\times2]} = bh \int_0^l {}^tE\,\underline{N}_{r,x}\,\underline{N}_{r,x}^T\,J\,d\hat{x} \tag{37}$$

$$\hat{\underline{K}}_{rb\ [2\times4]} = \hat{\underline{K}}_{br\ [4\times2]}^T = -b \int_{-h/2}^{} \int_0^l {}^tE\,\underline{N}_{r,x}\,\underline{N}_{b,\hat{x}\hat{x}}^T\,t\,J\,d\hat{x}\,dt = 0 \tag{38}$$

$$\hat{\underline{K}}_{bb\ [4\times4]} = \frac{bh^3}{12} \int_0^l {}^tE\,\underline{N}_{b,\hat{x}\hat{x}}\,\underline{N}_{b,\hat{x}\hat{x}}^T\,J\,d\hat{x} + S \int_0^l \underline{N}_{b,x}\,\underline{N}_{b,x}^T\,d\hat{x} \tag{39}$$

Since the second term in the right hand side of eqn (39) can be integrated by hand, the element stiffness matrix for the element with rectangular cross section is expressed in matrix form by

$$\hat{\underline{K}}_{(6\times6)} = \begin{bmatrix} \hat{\underline{K}}_{rr\ (2\times2)} & \hat{\underline{K}}_{rb\ (2\times4)} \\ \hat{\underline{K}}_{br\ (4\times2)} & (\hat{\underline{K}}_{bb}^n + \hat{\underline{K}}_{bb}^b)_{(4\times4)} \end{bmatrix}$$

$$= \begin{bmatrix} \hat{K}_{rr11} & \hat{K}_{rr12} & 0 & 0 & 0 & 0 \\ \hat{K}_{rr21} & \hat{K}_{rr22} & 0 & 0 & 0 & 0 \\ 0 & 0 & \hat{K}_{bb11}^n + \hat{K}_{bb11}^b & \hat{K}_{bb12}^n + \hat{K}_{bb12}^b & \hat{K}_{bb13}^n + \hat{K}_{bb13}^b & \hat{K}_{bb14}^n + \hat{K}_{bb14}^b \\ 0 & 0 & \hat{K}_{bb21}^n + \hat{K}_{bb21}^b & \hat{K}_{bb22}^n + \hat{K}_{bb22}^b & \hat{K}_{bb23}^n + \hat{K}_{bb23}^b & \hat{K}_{bb24}^n + \hat{K}_{bb24}^b \\ 0 & 0 & \hat{K}_{bb31}^n + \hat{K}_{bb31}^b & \hat{K}_{bb32}^n + \hat{K}_{bb32}^b & \hat{K}_{bb33}^n + \hat{K}_{bb33}^b & \hat{K}_{bb34}^n + \hat{K}_{bb34}^b \\ 0 & 0 & \hat{K}_{bb41}^n + \hat{K}_{bb41}^b & \hat{K}_{bb42}^n + \hat{K}_{bb42}^b & \hat{K}_{bb43}^n + \hat{K}_{bb43}^b & \hat{K}_{bb44}^n + \hat{K}_{bb44}^b \end{bmatrix} \tag{40}$$

where

$$\hat{\underline{K}}_{bb}^b = \frac{S}{10l} \begin{bmatrix} 12 & l & -12 & l \\ l & 4l^2/3 & -l & -l^2/3 \\ -12 & -l & 12 & -l \\ l & -l^2/3 & -l & 4l^2/3 \end{bmatrix} \tag{41}$$

and $\hat{K}_{rrij}(i,j=1,2)$ and $\hat{K}_{bbij}(i,j=1,2,3,4)$ are respectively the components of the submatrices $\hat{\underline{K}}_{rr}$ and $\hat{\underline{K}}_{bb}$.

2.5 Element External Nodal Forces

To evaluate the external nodal force vectors $\hat{\underline{f}}_r$ and $\hat{\underline{f}}_b$, the nodal virtual displacements $\delta\hat{\underline{u}}_r$ and $\delta\hat{\underline{u}}_b$ are introduced and the work done by the $\hat{\underline{f}}_r$ and $\hat{\underline{f}}_b$ going through the virtual displacement $\delta\hat{\underline{u}}_r$ and $\delta\hat{\underline{u}}_b$ is equated to the work done δW due to externally applied forces :

$$\delta W = \delta\hat{\underline{u}}_r^T\,\hat{\underline{f}}_r + \delta\hat{\underline{u}}_b^T\,\hat{\underline{f}}_b \tag{42}$$

in which the transposes of $\hat{\underline{f}}_r$ and $\hat{\underline{f}}_b$ are given by

$$\hat{\underline{f}}_r^T = [\,f_{x_1}\ \ f_{x_2}\,] \tag{43}$$

$$\hat{\underline{f}}_b^T = [\,f_{y_1}\ \ \hat{m}_1\ \ f_{y_2}\ \ \hat{m}_2\,] \tag{44}$$

where f_{xi} f_{yi} and $\hat{m}_i(i=1,2)$ are respectively the axial nodal forces, lateral nodal forces and moments due to externally applied forces at node i.

Since we use the incremental load in the present procedure, we assume that the load increment at each step is all the same. Considering the vertical and horizontal uniform loads W_n^0 and W_s^0 applied along the straight frame element, respectively, in the initial configuration as shown in Figure 3(a), we have

$$R_n^0 = W_n^0\,l^0\,, \quad R_s^0 = W_s^0\,l^0 \tag{45}$$

where R_n^0, R_s^0 and l^0 are respectively the total applied forces and initial element length. Since the geometry shape and length of the element in the current configuration have been changed by deformation, the magnitude of uniform load at time t is modified by

$$W_n = R_n / \int_0^l J\, d\hat{x}, \quad W_s = R_s / \int_0^l J\, d\hat{x} \tag{46}$$

where Jacobian J is given in eqn (36).

On the basis of constant incremental load at each step, we now consider two kinds of applied forces : one is the force whose direction maintains the same, the other is the force whose direction changes. From the first case as shown graphically in Figure 3(b), we obtain

$$W_{nx} = W_n \sin\theta_g, \quad W_{ny} = W_n \cos\theta_g \tag{47a}$$

$$W_{sx} = W_s \cos\theta_g, \quad W_{sy} = -W_s \sin\theta_g \tag{47b}$$

where W_{nx}, W_{ny}, W_{sx} and W_{sy} are respectively the $\hat{x}$ and $\hat{y}$ components of W_n and W_s and θ_g is the angle between global and local coordinates. Hence, we express the external virtual work in the current configuration by

$$\delta W = \int_C (W_{nx}+W_{sx})\delta\hat{u}\, dC + \int_C (W_{ny}-W_{sy})\delta\hat{v}\, dC \tag{48}$$

Substituting $\delta\hat{u}=\underline{N}_r^T\delta\hat{u}_r$ $\delta\hat{v}=\underline{\hat{N}}_b^T\,\delta\hat{u}_b$ and $dC=J\,d\hat{x}$ into eqn (46), we have $\delta W=\delta\underline{u}_r^T\int_0^l (W_{nx}+W_{sx})\ \underline{N}_r\ J\ d\hat{x}+\delta\underline{u}_b^T\int_0^l (W_{ny}-W_{sy})\ \underline{N}_b\ J\ d\hat{x}$

$$\delta W = \delta\underline{\hat{u}}_r^T \int_0^l (W_{nx}+W_{sx})\ \underline{N}_r\ J\ d\hat{x} + \delta\underline{\hat{u}}_b^T \int_0^l (W_{ny}-W_{sy})\ \underline{N}_b\ J\ d\hat{x} \tag{49}$$

Equating eqns (42) and (49), we have

$$\hat{\underline{f}}_r = \int_0^l (W_{nx}+W_{sx})\ \underline{N}_r\ J\ d\hat{x} \tag{50a}$$

$$\hat{\underline{f}}_b = \int_0^l (W_{ny}-W_{sy})\ \underline{N}_b\ J\ d\hat{x} \tag{50b}$$

If we consider W_n and W_s as the concentrated forces applied in the current configuration, the external nodal forces become

$$\hat{\underline{f}}_r = \int_0^l (W_{nd}+W_{sd})\ \underline{N}_r\ J\ \delta_d(\hat{x}-\hat{x}_d)\ d\hat{x} \tag{51a}$$

$$\hat{\underline{f}}_b = \int_0^l (W_{nd}-W_{sd})\ \underline{N}_b\ J\ \delta_d(\hat{x}-\hat{x}_d)\ d\hat{x} \tag{51b}$$

where $\hat{x}_d$ is the location of applied load and δ_d $(\hat{x}-\hat{x}_d)$ represents the Dirac delta function, defined by

$$\int_0^l \delta_d(\hat{x}-\hat{x}_d)\ d\hat{x} = 0 \quad for\ \hat{x} \neq \hat{x}_d$$

$$\int_0^l \delta_d(\hat{x}-\hat{x}_d)\ d\hat{x} = 1 \quad for\ \hat{x} = \hat{x}_d$$

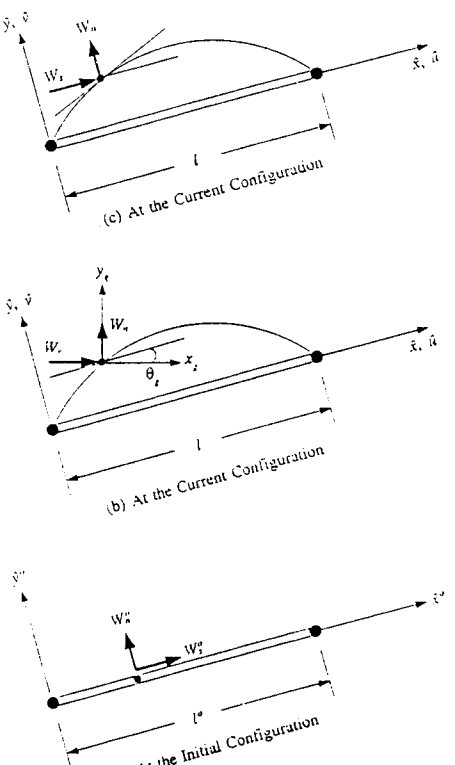

Figure 3 A Frame Element with External Loads

From the second case as shown in Figure 3 (c), we obtain the external virtual work in a similar manner of deriving eqn (49) by

$$\delta W = \delta \underline{\hat{u}}^T \int_0^l W_s \underline{N}_s J \, d\hat{x} + \delta \underline{\hat{u}}^T \int_0^l W_n \underline{N}_n J \, d\hat{x} \qquad (52)$$

Equating eqn (42) to eqn (52), we obtain the external nodal forces by

$$\hat{f}_s = \int_0^l W_s \underline{N}_s J \, d\hat{x} \qquad (53a)$$

$$\hat{f}_n = \int_0^l W_n \underline{N}_n J \, d\hat{x} \qquad (53b)$$

Similar to eqn (51), when W_n and W_s are considered as concentrated forces the external nodal forces may be evaluated from eqn (53) using Dirac delta function

2.6 Evaluation of Element Integral

To compute the element integral, Gaussian numerical integration is considered. For one-dimensional case, it is generally expressed by

$$I = \int_a^b f(\hat{x}) \, d\hat{x} = \frac{b-a}{2} \sum_{i=1}^{n} \omega_i f(\hat{x}_i) \qquad (54)$$

where n, ω_i and $\hat{x}_i$ are respectively the number of Gauss sampling points, the integration weight for the interval a to b and the location of Gauss sampling point. In eqn (54), the location $\hat{x}_i$ on the interval a to b is given by

$$\hat{x}_i = \frac{b+a}{2} + \frac{b-a}{2} r_i \qquad (55)$$

where r_i is a sampling point.

In evaluating integral for the element stiffness and nodal forces in the present study, the interval used to from 0 to l and the maximum integration order of $\hat{x}$ is five, by product of the displacement shape functions of a beam and Jacobian J. Since Gaussian numerical integration which uses n Gauss sampling points is exact if the integrand is a polynomial of degree of $2n-1$ or less, 3 may be adoptable as a n value.

2.7 Coordinate transformation

In this study, local coordinates are chosen to represent the individual element at every step. Each element formulation is then transformed from local coordinates to a set of convenient reference coordinates, i.e, global coordinates. Therefore, the applied forces, boundary conditions, and the displacements are uniquely expressed in terms of global coordinates.

Figure 4 shows an arbitrary oriented beam element and the two coordinate systems. The nodal displacements in terms of local coordinates and global coordinates are related by

$$\begin{bmatrix} \hat{u}_1 \\ \hat{v}_1 \\ \hat{\theta}_1 \\ \hat{u}_2 \\ \hat{v}_2 \\ \hat{\theta}_2 \end{bmatrix} = \begin{bmatrix} \lambda & \mu & 0 & 0 & 0 & 0 \\ -\mu & \lambda & 0 & 0 & 0 & 0 \\ 0 & 0 & 1 & 0 & 0 & 0 \\ 0 & 0 & 0 & \lambda & \mu & 0 \\ 0 & 0 & 0 & -\mu & \lambda & 0 \\ 0 & 0 & 0 & 0 & 0 & 1 \end{bmatrix} \begin{bmatrix} u_1 \\ v_1 \\ \theta_1 \\ u_2 \\ v_2 \\ \theta_2 \end{bmatrix} \qquad (56a)$$

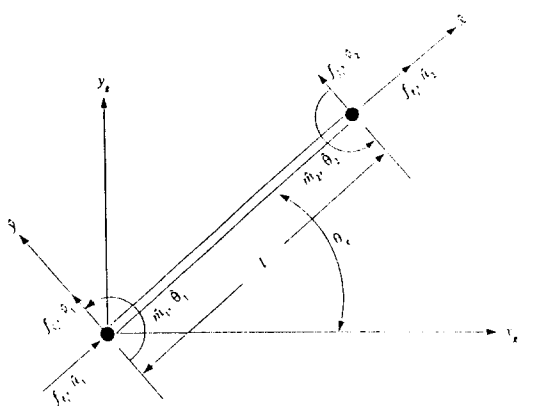

Figure 4 Arbitrarily Oriented Beam Element

or symbolically

$$\hat{d} = T\, d \tag{56b}$$

where $\lambda=\cos\theta_g$ and $\mu=\sin\theta_g$ with θ_g being the angle of orientation of the beam as shown in Figure 4. Similarly, the external nodal forces in the terms of local coordinates and global coordinates are related by

$$\hat{f} = T f \tag{57}$$

where the transposes of and are given by

$$\hat{f}^T = [\, f_{\hat{x}_1} \;\; f_{\hat{y}_1} \;\; \hat{m}_1 \;\; f_{\hat{x}_2} \;\; f_{\hat{y}_2} \;\; \hat{m}_2 \,] \tag{58a}$$

$$f^T = [\, f_{x_1} \;\; f_{y_1} \;\; m_1 \;\; f_{x_2} \;\; f_{y_2} \;\; m_2 \,] \tag{58b}$$

Arranging eqn (40) according to the corresponding six nodal degrees of freedom and considering the external nodal forces, (the nodal) force-displacement relationship is obtained by

$$\begin{bmatrix} f_{\hat{x}_1} \\ f_{\hat{y}_1} \\ \hat{m}_1 \\ f_{\hat{x}_2} \\ f_{\hat{y}_2} \\ \hat{m}_2 \end{bmatrix} = \begin{bmatrix} \hat{K}_{rr11} & 0 & 0 & \hat{K}_{rr12} & 0 & 0 \\ 0 & \hat{K}_{bb11}^n + 6S/(5l) & \hat{K}_{bb12}^n + S/10 & 0 & \hat{K}_{bb13}^n - 6S/(5l) & \hat{K}_{bb14}^n + S/10 \\ 0 & \hat{K}_{bb21}^n + S/10 & \hat{K}_{bb22}^n + 2Sl/15 & 0 & \hat{K}_{bb23}^n - S/10 & \hat{K}_{bb24}^n - Sl/30 \\ \hat{K}_{rr21} & 0 & 0 & \hat{K}_{rr22} & 0 & 0 \\ 0 & \hat{K}_{bb31}^n - 6S/(5l) & \hat{K}_{bb32}^n - S/10 & 0 & \hat{K}_{bb33}^n + 6S/(5l) & \hat{K}_{bb34}^n - S/10 \\ 0 & \hat{K}_{bb41}^n + S/10 & \hat{K}_{bb42}^n - Sl/30 & 0 & \hat{K}_{bb43}^n - S/10 & \hat{K}_{bb44}^n + 2Sl/15 \end{bmatrix} \begin{bmatrix} \hat{u}_1 \\ \hat{v}_1 \\ \hat{\theta}_1 \\ \hat{u}_2 \\ \hat{v}_2 \\ \hat{\theta}_2 \end{bmatrix} \tag{59a}$$

or symbolically

$$\hat{f} = \hat{K}_m\, \hat{d} \tag{59b}$$

Substituting eqns (56b) and (57) into eqn (59b), and considering the orthogonal property of the transformation matrix, we obtain

$$f = K_m\, d \tag{60}$$

where K_m is the transformed element stiffness matrix in terms of global coordinates:

$$K_m = T^T \hat{K}_m\, T \tag{61}$$

The total stiffness matrix can now be assembled for the entire elements by using the direct stiffness method. When the total stiffness matrix has been assembled, the external global nodal forces are related to the global nodal displacement. Introducing the boundary conditions, all unknown variables are evaluated.

3. NUMERICAL EXAMPLES

To validate the presented formulation and demonstrate the importance of imposing material properties properly, examples of cantilever beams and frame are considered.

3.1 Cantilever Beam with End Forces

The large deformation behavior of the cantilever beam with end force shown in Figure 5 is studied. To this end, two loading conditions are considered: case one considered a vertical non-conservative force P_v of 8 KN and case two considered a horizontal force P_h of 30000 KN. This beam is discretized by five equal elements. The results are shown in Figures 6, 7 and 8.

Figure 6 showns good agreement between the solutions of the present study and Ref.

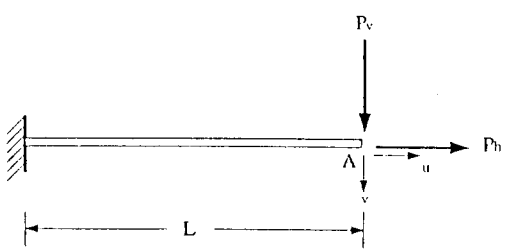

Figure 5 Cantilever Beam with Concentrated End Forces : L=10 m, h=0.1 m, b=1 m, ^oE=1.2 KN/ mm^2, $^o\nu$=0.0.

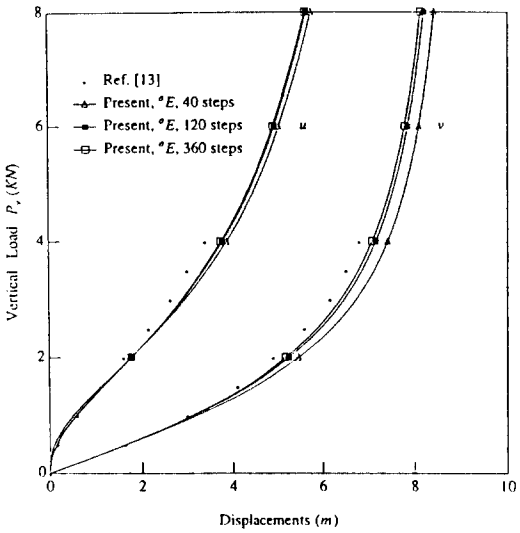

Figure 6 Horizontal and Vertical Displacements of the Cantilever Beam under Load P_v

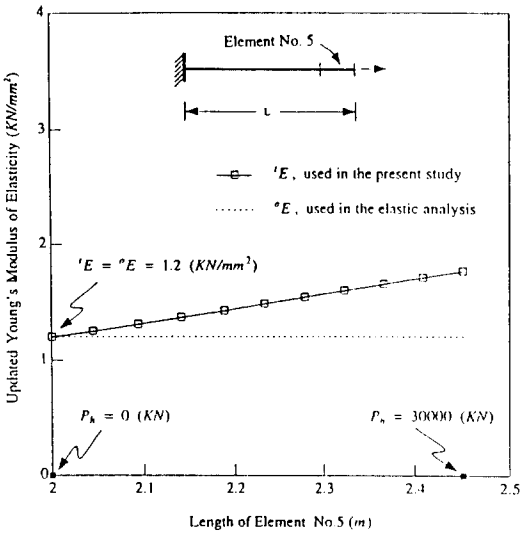

Figure 8 Updated Young's Modulus of Elasticity in Element No. 5 of the Cantilever Beam under Load P_h

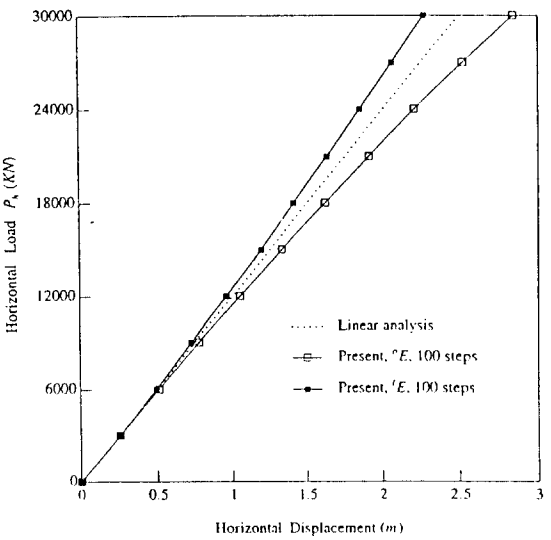

Figure 7 Horizontal and Vertical Displacements of the Cantilever Beam under Load P_h

[13] and shows that the explicit solutions are very stable and converges rapidly as the number of increment loading steps increase. the increase in accuracy is due to the fact that the geometry of the deformed cantilever is updated more accurately with a larger number of incremental load steps. In Figure 7, the results obtained by considering a) updated material properties and updated geometry and b) updated geometry only are compared with that by linear analysis for the second loading case. Since the stiffness of a beam element, which is considered to have the same material properties and cross-section area during deformation, becomes softer and softer when it is gradually elongated, the axial displacement should be larger and larger. However, the stiffness of a beam element subjected to incremental tensile loadings becomes stiffer and stiffer in real situation. The results obtained by present formulation show exactly the same way. In Figure 8, the updated Young's modulus of elasticity ^tE is evaluated for the element No.5 of the cantilever beam which is subjected to the horizontal load P_h. It shows that the updated Young's modulus of elasticity of the element becomes bigger when the element becomes elongated.

3.2 Cantilever Beam with End Moment

A cantilever beam with two different properties subjected to a concentrated moment M

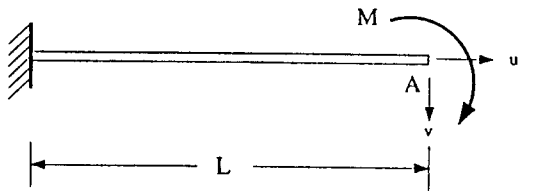

Figure 9 Cantilever Beam with an End Moment :
(a) L=100 in, b=1.0 in, h=0.5 in, $^0E=1.2\times10^4$ l b/ in^2, $^0\nu=0.0$;
(b) L=12 in, b=1.0 in, h=1.0 in, $^0E=30\times10^6$ l b/ in^2, $^0\nu=0.0$.

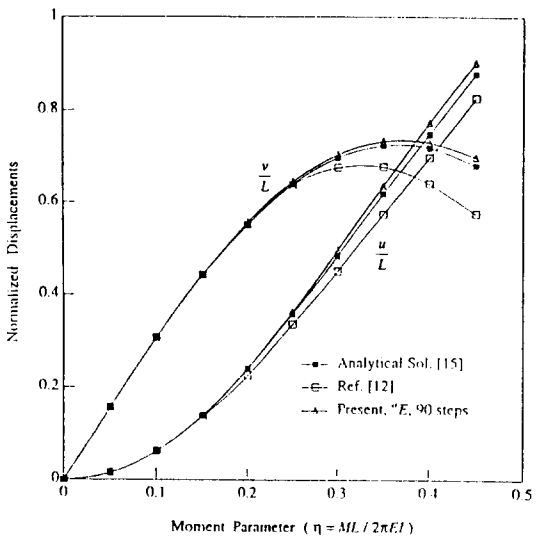

Figure 10 Load-Displacement Curves of the Cantilever Beam (a) under End Moment

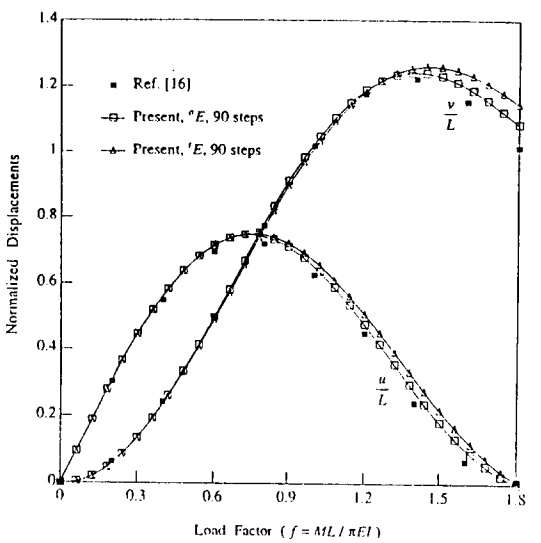

Figure 11 Load-Displacement Curves of the Cantilever Beam (b) under End Moment

at the free end as shown in Figure 9 is considered. This beam is discretized by twenty elements for case(a) and twelve elements for case(b). The results are shown in Figures 10, 11 and 12.

In Figures 10 and 11, the plots of normalized displacements versus moment parameter and load factor f for the tip of the beam are shown. Results are compared with those of Refs. [2] and [4] in Figure 10 for case(a), and of Ref. [7] in Figure 11 for case(b). IN Ref. [12], ADINA was used with 90 incremental load steps, 20 beam elements, and no equilibrium iterations. In Ref. [16], total Lagrangian approach with incremental interations is used to handle geometrically nonlinear three dimensional beam problems. The results from above two figures show that the predicted response compares well with the analytical and numerical solutions respectively given in Refs. [15] and [16]. Figure 12 shows the deformed shapes of the cantilever beam obtained by the presented method for case(b) for the maximum load of f=1.8 with 90 incremental load steps

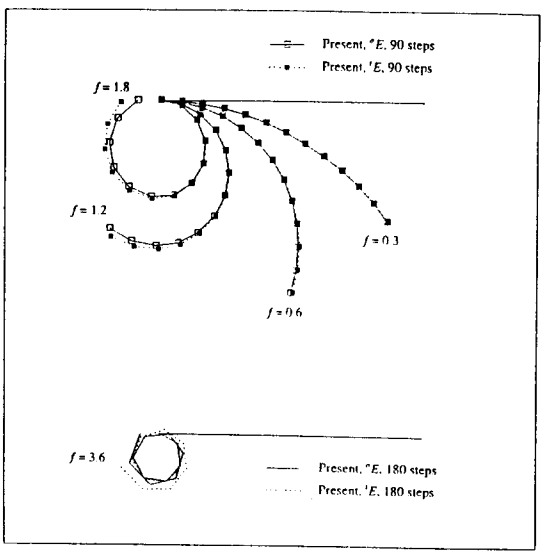

Figure 12 Deformed Shapes of Cantilever Beam (b)

and f=3.6 with 180 incremental load steps. From the deformation shapes of the beam, we may see the differences of the results by ${}^0E$ and ${}^tE$ and the capabilities of handling large displacement and large rotation problems.

3.3 Diamond-Shaped Frame

A diamond-shaped frame composed of four equal bars and loaded by forces applied at a pair of diagonally opposite joints as shown in Figure 13 is analyzed. The two loaded joints are assumed to be hinged while the two free joints are assumed to be rigid. A quarter of the frame is modeled by ten equal elements. The results are shown in Figures 14 and 15.

In Figures 14 and 15, the plots of normalized displacements versus load factors under tensile and compressive loadings are shown. Since the member strain of the frame is very small, Young's modulus of elasticity ${}^0E$ is only considered. Results are compared with those of Ref. [21], where analytical solutions with experimental results for this frame are provided. From the figures, we see that the solutions show excellent agreements with theory[21].

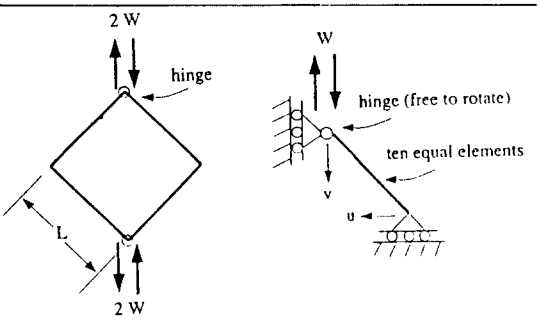

Figure 13 Diamond-Shaped Frame Structure : L=17 in, b=1.0 in, h=0.0625 in, ${}^0E=28.95\times10^6$ lb/ in^2, ${}^0\nu=0.0$.

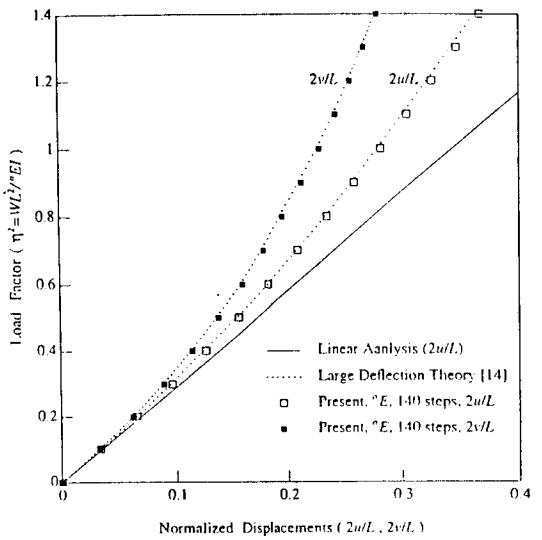

Figure 14 Vertical and Horizontal Displacements of the Frame under Tensile Loading

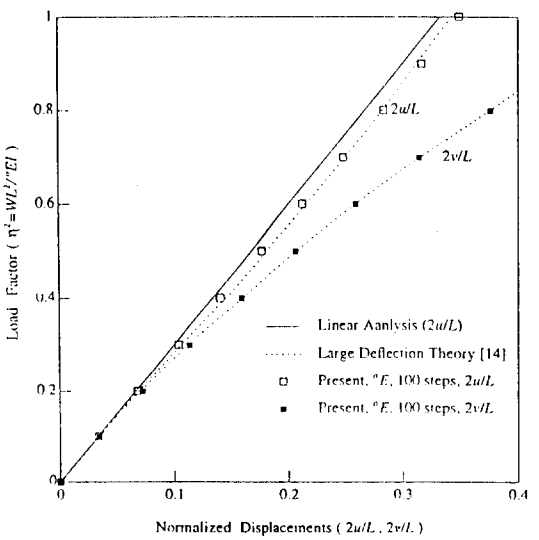

Figure 15 Vertical and Horizontal Displacements of the Frame under Compressive Loading

4. SUMMARY AND CONCLUSIONS

This paper presents an explicit finite element nonlinear formulation for very large deformations of plane frame structures. The formulation is based on an updated material reference frame and hence a true stress-strain test can be directly applied to characterize the properties of material which is subjected to very large deformations. The co-rotational approach, by which the major geometric nonlinearities are embodied in the coordinate transformation when element assemblage is formed, is adopted. The element stiffness matrix is obtained by superimposing the bending and

geometric stiffness matrices of the linear bar element is a body attached coordinate.

It has been demonstrated by the examples that the present formulation has the capability of handling very large geometric changes. In addition, the incremental numerical procedure has shown to be very stable and converges rapidly when small load or deformation increments are used. The importance of using proper material properties in large deformation analysis has also been demonstrated.

REFERENCES

1. Hibbit, H.D., Marcal, P.V. and Rice, J.R., "A Finite Element Formulation for Problems of Large Strain and Large Displacement", *Int. J. Solids Structures*, Vol. 6, pp.1069-1086, 1970.
2. Ramm, E., "A Plate /Shell Element for Large Deflections and Rotations", *In Formulations and Computational Algorithms in Finite Element Analysis*, (Eds. K.J. Bathe, J.T. Oden and W. Wunderich), MIT Press, 1977.
3. Wood, Arches and Zienkiewicz, O.C., "Geometrically Nonlinear Finite Element of Beams, Frames, Arches and Axisymmetric Shells", *Comput. Struct.*, Vol. 7, pp.725-735, 1977.
4. Bathe, K.J. and Bolourchi, S., "Large Displacement Analysis of Three-Dimensional Beam Structures", *Int. J. Numer. Meth. Engng.*, Vol. 14, pp.961-986, 1979.
5. Remseth, S.N., "Nonlinear Static and Dynamic Analysis of Framed Structures", *Comput. Struct.*, Vol. 10, pp.879-897, 1979.
6. Oliver, J. and Onate, E., "A Total Lagrangian Formulation for the Geometrically Nonlinear Analysis of Structures using Finite Elements. Part Ⅱ: Arches, Frames and Axisymmetric Shells", *Int. J. Numer. Meth. Engng.*, Vol. 23, pp.253-274, 1986.
7. Surana, K.S. and Sorem, R.M., "Geometrically Non-linear Formulation for Three Dimensional Curved Beam Elements with Large Rotations", *Int. J. Numer. Meth. Engng.*, Vol. 28, pp.43-73, 1989.
8. Wen, R.K. and Rahimzadeh, J., "Nonlinear Elastic Frame Analysis by Finite Element", *J. Struct. Engng., ASCE*, Vol. 109, pp.1952-1971, 1983.
9. Peterson, A. and Petersson, H., "On finite Element Analysis of geometrically Nonlinear Problems", *Comput. Meth. Appl. Mech. Engng.*, Vol. 51, pp.227-286, 1985.
10. Wong, M.B. and Tin-Loi, F., "Geometrically Nonlinear Analysis of Elastic Framed Structures", *Comput. Struct.*, Vol. 34, pp. 633-640, 1990.
11. Wempner, G., "Finite Elements, Finite Roatations and Small Strains of Flexible Shells", *Int., J., Solids Structures*, Vol. 6, pp. 117-153, 1969.
12. Oran, C. and Kassimali, A., "Large Deformations of Framed Structures under Stratic and Dynamic Loads", *comput. Struct.*, Vol. 6, pp.539-547, 1976.
13. Horrigmoe, G. and Bergan, P.G., "Nonlinear Analysis of Free-form Shells by Flat Finite Elements", *Comput. Meth. Appl. Mech. Engng.*, Vol. 16, pp.11-35, 1978.
14. Belytschko, T. and Glaw,m L.W., "Applications of Higher Order Co-rotational Stretch Theories to Nonlinear Finite Element Analysis", *Compt. Struct.*, Vol. 10, pp.175-182, 1979.
15. Mattiason, K., "On the Co-rotational Finite Element Formulation for Large Deformation Problems", *Publication 83:1, Dept. of Structural Machanics*, Chalmers Univ. of Technology, 1983.
16. Hsiao, K.M. and Hou, F.Y., "Nonlinear Finite Element Analysis of Elastic Frames", *Comput. Struct.*, Vol. 26, pp.693-701, 1986.
17. Rankin, C.C. and Brogan, F.A., "An Element Independent Co-rotational Procedure for the Treatment of Large Rotations", *J. Press. Vessel Technol, ASME*, Vol. 108, pp.165-174, 1986.
18. Hsiao, K.K., Horng, H.J. and Chen, Y.R., "A Corotational Procedure that Handles Large

Rotations of Spatial Beam Structures", *Comput. Struct.*, Vol. 27, pp.769-781, 1987.

19. Crisfield, M.A. and Cole, G., "Co-rotational Beam Elements for Two-and Three-Dimensional Non-linear Analysis", *Discretisation Meth. in Strut. Mech.*, ed. G. Kuhn et al., Springer-Verlag, pp.45-124, 1989.
20. Crisfield, M.A., "A Consistent Co-ratational Formulation for Non-linear, Three-Dimensional Beam Elements", *Comput. Mech. Appl. Mech. Eng.*, Vol. 81, pp.131-150, 1990.
21. Jenkins, J.A., Seitz, T.B. and Przemieniecki, J.S., "Large Deflections of Diamond Shaped Frames", *Int. J. Solids Structures*, Vol. 2, pp. 591-603, 1966.
22. Yun, Y.M., "An Explicit Finite Element Formulation for Very Large Deformations Based on Updated Material reference Frame", *Finite Elements in Analysis and Design*, Vol. 13, pp. 209-224, 1993.

(접수일자 1994. 7. 11)

APPENDIX : Conversion Factors

1 in=25.4 mm	1 in2=645.2 mm2
1 kip=4.448 KN	1 ksi=6.895 MPa